Design of a passive photonic integrated circuit for QKD

Pedro Ricardo Neto Mendes
pedro.neto.mendes@tecnico.ulisboa.pt

Instituto Superior Técnico, Lisboa, Portugal

December 2020

Abstract

Information is one of the most fundamental resources in our world. To keep it safe, quantum key distribution is being developed and implemented all over the world. In Portugal, a proof-of-principle implementation has been done. Now, to take it to the next level, it must be made more resilient, robust and efficient. This thesis approaches this aim intending to design a new system that improves on the current one and will be possible to refine in the future. To do this, femtosecond laser fabrication is analysed as a fabrication method for a passive photonic integrated circuit capable of performing QKD. This process shows great potential to produce such a device. The device is designed step by step from waveguides to directional couplers. A blueprint for the photonic circuit is proposed. While not fabricated and tested, by comparison to other works, it would work, although some interactions would be necessary to reach its maximum efficiency. In addition, a new photon source was explored. A full experimental characterization is being made based on the theoretical study and simulations presented here.

Keywords: Quantum Information, Photonics, Integrated Optics, Waveguide Optics, Nonlinear Optics.

1. Introduction

It is believed that we are now amid the second quantum revolution. The discovery and development of quantum mechanics marked the first quantum revolution. We used quantum mechanics to understand what already existed. We could explain how metals and semiconductors behaved, but not control or manipulate that behavior. Inventions such as the laser and the transistor, the basic building block of computers, were built following these rules. This approach has given us many of the core technologies underpinning modern society.

The second quantum revolution aims at applying quantum mechanics in every aspect of our lives. The difference between science and technology is the ability to engineer your surroundings to your own ends, and not just explain them. We go from passive observers of the quantum world to actively employing quantum mechanics to alter the world. For example, besides explaining the periodic table, we can make new artificial atoms - quantum dots and excitons - which we can engineer to have electronic and optical properties of our own choosing.

Thus, although quantum mechanics as a science has matured substantially, quantum engineering as a technology is now emerging on its own right. We can divide quantum technology into three main sub-fields, quantum computing, quantum metrology and quantum communication.

Information is an essential resource to everyone and to the current society. As such, communication is then a key aspect of our lives, as it is the way we exchange information between two parties. In order to guarantee the security of any communication, QKD can be used. Quantum Key Distribution protocols have attracted a lot of attention since the first proposal in 1984 [1]. QKD is a secure communication method which implements a cryptographic protocol making use of the principles of quantum physics. It enables two parties to produce a shared random secret key known only to them, which can then be used to encrypt and decrypt messages.

This revolution is of great importance to the entire world, and therefore there are efforts from many countries and groups to lead and have a powerful presence. In Europe, the Quantum Technologies Flagship launched in October 2018 has an expected budget of 1 billion euros over ten years to support the work of quantum researchers [2].

1.1. State-of-the-art

At present, QKD systems are commercially available. These systems currently rely mostly on attenuated laser pulses rather than single photons. Before QKD can be widely adopted, it faces several important challenges such as secret key rate, distance, size, cost and practical security [3].

Recently, Satellite Quantum Key Distribution

(SatQKD) has proved to be able to overcome the range limits, enabling secure communication globally. The Chinese mission, known as Micius [4], successfully demonstrated various quantum communication protocols in space [5]. Furthermore, satellites smaller and cheaper than Micius, such as nanosatellites (with a mass ≈10 kg) have been in the spotlight [6], for the possibility of establishing quantum communication services using a constellation [7].

The need to integrate QKD into these nanosatellites and into novel applications gave rise to the miniaturization of devices for free-space quantum key distribution. Integration of controlled phase shifters in integrated interferometers has been used to control single-photon qubit states, manipulate multi-photon entangled states of up to four photons and demonstrate on-chip quantum metrology [8].

However, an efficient route to high-speed encoding of the quantum phase states on chip is still missing. In [9], a novel approach to high-speed phase encoding is exploited and a compact, scalable and power efficient integrated quantum transmitter is demonstrated. A secure key rate of 270 kHz is achieved with a chip size of 6x2 mm^2.

An alternative fabrication technique, femtosecond laser direct writing, based on laser writing has been demonstrated [10]. It promises rapid prototyping and enables maskless high resolution three-dimensional fabrication of integrated optical devices.

In [11], an optical architecture of 35x20x8 mm^3 is proposed. In this work the polarization is controlled for each diode's emission by a wire-grid polariser and the spatial overlap accomplished by a femtosecond fabricated device. Tests with a free-space receiver indicated an average error ratio of 3.3 % and an asymptotic secure key rate of 54 kHz under static alignment.

The approach presented in this papers follows from this work but tries to integrate the control of the polarization in the femtosecond laser written device.

1.2. Motivation

While there are many ways of working with quantum systems, photons are chosen for this work. A photon's multiple degrees of freedom can be prepared in distinct states and manipulated using conventional optical components such as waveplates and beamsplitters. Furthermore, photons do not interact with one another or with the environment meaning that noise due to a quantum state interacting with its surroundings is virtually eliminated.

Nevertheless, using these conventional components, the size of the devices becomes too big for small scale applications. To overcome this problem, quantum circuits, similar to electronic circuits, can be developed. Furthermore, the ability to have high density complex designs has encouraged the on-chip integration of photonic quantum circuits.

This thesis work is part of a bigger project with the ultimate goal of realizing satellite-to-ground quantum key distribution. In order to do this, an approach that would allow the miniaturization and improvement of the current quantum key distribution setup was developed while also studying how to make it better suited to perform satellite-to-ground quantum key distribution.

In addition, a new photon source was explored to implement new protocols, to investigate new applications and to improve the current one.

2. Quantum Key Distribution - From protocols to systems

The state of a qubit can be encoded in the polarization of a photon. By convention, the horizontal polarization ($|H\rangle$) is defined as the $|0\rangle$ state and the vertical polarization ($|V\rangle$) as the $|1\rangle$ state. Any polarization can be given by a superposition of these two, as any state is the superposition of $|0\rangle$ and $|1\rangle$. This basis is the standard basis Z=$|H\rangle$,$|V\rangle$ but the qubits can also be written in other common basis such as X=$|D\rangle$,$|A\rangle$ and Y=$|R\rangle$,$|L\rangle$.

In order to access the information stored in the qubit, one has to measure it. When making a measurement, a basis must be chosen. The result will be one of the states that generates that basis. This is an important result from quantum mechanics.

Since the state of the qubit might not be one of the states of the basis chosen, the result is probabilistic in nature. For example, if the initial state is the diagonal polarization, $|D\rangle$, and the basis chosen is the Z basis, the probability of measuring an horizontal polarization, $|H\rangle$, corresponding to a bit value of 0 is given by:

$$\begin{aligned} P(|H\rangle) = |\langle D|H\rangle|^2 &= \left|\frac{1}{\sqrt{2}}\left(\langle H| + \langle V|\right)|H\rangle\right|^2 \\ &= \left|\frac{1}{\sqrt{2}}(\langle H|H\rangle + \langle V|H\rangle)\right|^2 = \left|\frac{1}{\sqrt{2}}(1+0)\right|^2 \\ &= \frac{1}{2}. \end{aligned} \tag{1}$$

This result means that there is a 50% chance of measuring a 0 and, therefore, a 50% chance of measuring a 1 if the measurement is made in Z basis and the state was in the diagonal polarization. After the measurement, the photon will be in the state measured, either horizontal or vertical polarization.

2.1. BB84 protocol

The BB84 protocol is one of the most widely used and simple QKD protocols. It is based on the mea-

surement properties discussed and on the fact that it is impossible to clone a quantum state.

In an ideal world (perfect equipment and no undesirable interactions with the environment), it has been mathematically proven to be secure against all classical and quantum attacks [12], as have other QKD protocols. In addition, Alice and Bob can detect any active attempt by an eavesdropper (E)ve to eavesdrop on the key distribution process.

Any type of communication is made between two parties, Alice and Bob in this case. In order to implement the BB84 protocol, Alice and Bob need to share a classical public communication channel and a quantum communication channel. A quantum channel is nothing more than a way to send and receive qubits. This could be for example an optical fiber or even free space. The steps of the protocol are as follows:

1. Alice begins by choosing a random string of bits

2. For each bit, a basis is randomly chosen between Z and X

3. Alice transmits each qubit to Bob over the quantum channel

4. Bob randomly chooses a basis in which to measure each qubit (Z or X basis)

5. Bob and Alice notify each other over any classical channel (even insecure ones) what basis they used to measure each qubit

6. Alice and Bob will discard the bits corresponding to the qubits measured in different basis

7. Alice and Bob should now have an identical string of random bits which is called a sifted key

The results measured in a different basis to that in which they were created are discarded because they cannot be predicted to be correct. If Alice sends a photon with an horizontal polarization and thus a bit with value 0, Bob can measure either diagonal or anti-diagonal polarization if he chooses to measure in the X basis. The probability will, in theory, be 50% of getting the correct result.

Otherwise, when Bob chooses the same basis as Alice, the probability of measuring the correct bit value is 100%. Therefore, these measurements are kept and will result in the creation of the final key.

As the probability of Bob choosing the same basis as Alice is 50%, only half of the bits sent will not be discarded, on average.

2.2. Spatial mode mixing with bulk optical components

Various different QKD protocols have been implemented using bulk optics in recent times. In 2019, the telecommunication institute of Portugal performed the first quantum communication experiment in the country using free-space propagation with a bulk optical approach. This experiment was a success. Nevertheless, in order to achieve better results and more practical applications, new ideas are being explored.

In order to implement the BB84 protocol, the emitter, Alice, has to be able to deterministically prepare one of four polarized states. These four states are, in this case, the horizontally polarized ($|H>$), the vertically polarized ($|V>$), the diagonally polarized ($|D>$) and the anti-diagonally polarized ($|A>$).

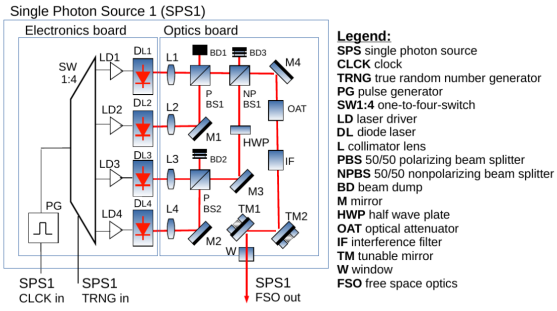

Figure 1: Schematic of the emitter (Alice) used for the BB84

In figure 1, a design for an emitter using bulk optics is presented. It can be seen that there are four inputs and one output. Each input is connected to the output through a different optical path, through different optical elements. These guarantee that each path has a different and determined polarization at the output. Therefore, by switching on only one of the diode lasers at each emission, one of the four polarized states is created at the output.

The diode lasers used here are not single photon sources, however, using filters to attenuate the intensity, weak coherent pulses are created. The average pulse rate can be controlled and is chosen in order to have one photon in most pulses while minimizing the likelihood of having two photons. This would leave the protocol open to attacks.

The design for the receiver is not shown, however, it is very similar to the emitter.

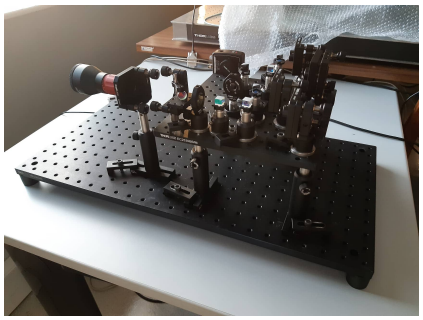

Figure 2: Optical setup of the emitter (Alice) used for the BB84 protocol.

Figure 2 shows the optical part of the emitter assembled in the lab. As it can be seen, it is too big and heavy for practical applications.

Most of the size comes from the optical part of the setup while the electronics can already be made to fit the requirements of small-scale applications.

3. Analysis of femtosecond laser fabrication for integrated photonic waveguides

Commonly, high density optical circuit fabrication is done using conventional technologies readily integrated with standard CMOS fabrication techniques. These fabrication techniques place some limitations on circuit design. Large scale production of waveguide patterns is done with either a chrome mask to selectively illuminate a photosensitive resist or alternatively electron beam lithography. This restricts the flexibility of the circuits.

The femtosecond laser direct-write technique is a unique way to produce glass waveguides. In recently years, femtosecond (fs) laser direct writing of transparent material has become a powerful microfabrication technique for passive and active integrated optical devices. The ability to create 3D optical or photonic devices by sequential direct-writing of individual devices can lead to more flexible, efficient and smaller quantum circuits.

The structure produced depends on laser parameters (pulse duration, wavelength, energy, repetition rate), material parameters (band gap, thermal expansion coefficient, etc.), and the numerical aperture (NA) of the focusing.

3.1. Background

When a femtosecond laser pulse is focused inside a transparent material, the optical intensity in the focal volume can become high enough to induce permanent structural modifications such as a refractive index change or the formation of a small vacancy.

The incident photons do not have enough energy to overcome the band gap energy of the dielectric materials. However, when the incident laser intensity is high enough, nonlinear optical effects are observed.

The first is photoionisation. This effect allows for electrons in the valence band to go to the conduction band as a result of tunnelling ionisation or multi-photon ionisation.

After the photoionisation process, there are some free electrons in the material. These electrons keep absorbing energy from the laser pulse and avalanche ionization occurs. The energetic free electrons kick the valence electrons to the conduction band giving rise to more free electrons. This results in an exponential increase on the number of free electrons.

In essence, a femtosecond laser pulse produces a strong nonequilibrium condition in a material with electron temperatures much higher than lattice temperatures. The result of the femtosecond laser on the material will then be the way the systems reacts to the nonequilibrium condition.

3.2. Modification regimes induced by laser intensity

To date, three qualitatively different kinds of structural changes have been induced in the bulk of transparent materials with femtosecond laser pulses. These modifications are characterized by the intensity of the laser and by the material properties. This can be seen in figure 3.

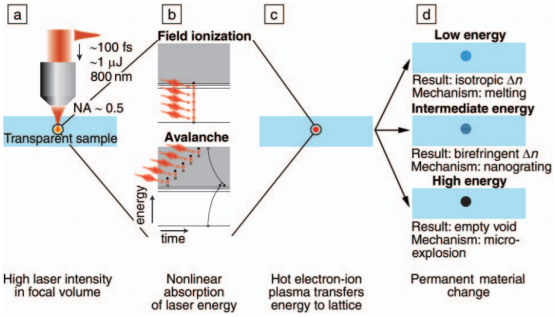

Figure 3: Schematic illustration of key steps in femtosecond-laser-induced structural change in bulk transparent materials. [13]

The smooth refractive index change, also known as Type I modification, is ideal for low loss waveguides. The refractive index of the material suffers an isotropic change on the focus spot of the laser. The reason behind this change is not yet fully understood but it is usually attributed to the combination of some different mechanisms.

In fused silica, the density increases if the glass is quenched from a high temperature, explaining the higher refractive index (typically on the order of 10^{-3}) observed in femtosecond laser irradiated fused silica [14].

At intermediate laser intensities, a non-isotropic index change has been observed, resulting in birefringence and negative refractive index change.

This means the waveguides supports guided modes with different propagation constants for two orthogonal polarization states. This allows the fabrication of waveguide segments capable of manipulating the polarization.

The appearance of birefringence can be the result of diverse effects, depending on the substrate material and the irradiation conditions. It is usually the result of ellipticity of the waveguide cross-section, mechanical stress in the modified region or laser-induced intrinsic birefringence.

Osellame et al. developed a simple technique to obtain a birefringent waveguide with tilted optical axis in [15]. A schematic design of this technique can be seen in figure 4.

They showed how this technique can be applied to the creation of an integrated device for quantum tomography of a two-photon state and the fabrication of components such as polarization insensitive and polarizing directional couplers [16].

Finally, when the laser intensity reaches critical values for the given material, the region of modification is characterised by material damage or void formation. This is caused by explosive expansion of highly excited, vaporized material out of the focal volume and into the surrounding material, a process called micro-explosion [17].

Voids have been used in for the fabrication of optical memory devices and other devices not interesting for this work.

3.3. Modification regimes induced by the laser's repetition rate

In addiction to the modifications caused in the material due to the intensity of the laser, the repetition rate also creates distinct regimes when fabricating photonic circuits. This is the result of possible overlap between the relaxation time of the material and the arrival of the next pulse, as can be seen in 5.

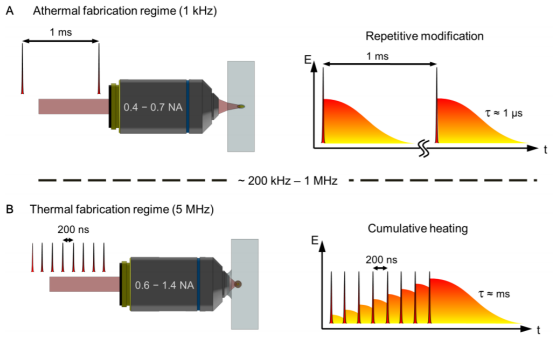

Figure 5: Schematic of the thermal regimes [18]

In the athermal regime where the time span between successive laser pulses is considerably longer than the thermal diffusion time of the glass, which is typically of the order of microseconds, a pulse-by-pulse repetitive modification of the material occurs. As a result of the low pulse repetition rate (<100 kHz), slow translation speeds, typically in the order of tens of micrometres per second are required in order to obtain sufficient spatial overlap between individual modifications to create a continuous waveguide.

In contrast, in the thermal regime, successive pulses arrive well below the thermal diffusion time of the material. Thus there is insufficient time between pulses for the heat to diffuse out of the focal volume and an accumulation of heat occurs. As a result of the high laser repetition rate, the sample can be translated at speeds of millimetres per second and thus the waveguide inscription is orders of magnitude quicker than in the athermal regime.

Furthermore, a volume of material much greater than the focal volume can be structurally altered, because if enough energy is absorbed, a volume of material larger than the focal volume can be heated above the melting temperature [19]. Also, due to symmetric thermal diffusion outside of the focal volume, a spherically shaped modified region is produced. In general, the thermal regime is more advantageous to create the devices necessary for photonic circuits.

3.4. Different writing configurations for waveguide inscription in glasses

In other to fabricate a waveguide or any other device using FLDW, the focal spot has to be moved through the material. Usually, the sample is placed on computer controlled motion control equipment to translate it in three dimensions with respect to the focal spot. The sample can either be translated parallel to the laser beam direction, the so-called longitudinal writing, or perpendicular to the laser beam, transverse writing as illustrated in figure 6.

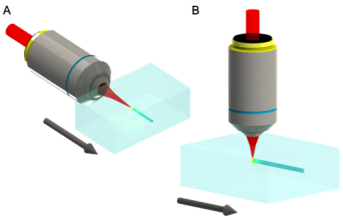

Figure 6: Schematic of inscription processes [18].

The longitudinal writing technique offers the advantage that the waveguides will be closer to circular in shape. However, the working distance of the objective lens limits the writing length of the waveguide.

The transverse writing geometry is more flexible. Structures can be fabricated within the bulk material, limited in size only by the positioning system,

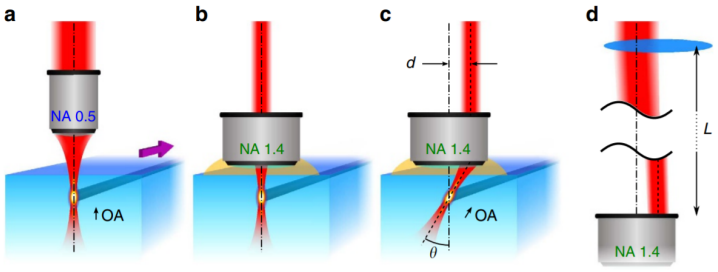

Figure 4: Conceptual scheme of the method enabling the direct writing of optical waveguides acting as integrated waveplates with tilted axis.[15]

while the maximum structure depth is determined by the working distance of the focusing objective. The main disadvantage, however, is the asymmetry of the produced structure.

Except for very high-NA objectives, the focal radius will always be much smaller than the confocal parameter, resulting in a waveguide with an elliptical cross section. However, there are techniques or conditions where this disadvantage can be mitigated making the transverse writing scheme the preferred one.

4. Design of a passive photonic integrated approach for QKD

Photonic integrated circuits are devices on which several optical (and often also electronic) components are integrated. In order to construct a photonic circuit capable of performing QKD, the design, analysis and optimization of various passive components was made. These designs were created with the intention of being produced using femtosecond laser fabrication.

4.1. Components

Waveguide

A waveguide is the fundamental element of integrated optics. It is used to guide electromagnetic waves through a device as electric wires are used to carry electric currents. Typical optical waveguides include the common optical fibers and other transparent dielectric waveguides made of plastic and glass. In most cases, light is confined in the core by total internal reflection.

Optical energy can be lost from guided modes by radiation, in which case photons are emitted into the media surrounding the waveguide. Radiation losses from either planar or straight channel waveguides are generally negligible for well confined modes. For this reason the losses in the straight waveguides are primarily due to fabrication and material imperfections and low compared to other photonic devices.

The transmission loss of highly purified glass has become as low as 0.15 dB/km at $\lambda = 1.55$ μm.

Nevertheless, waveguides fabricated by femtosecond laser direct writing tend to have greater propagation losses due to the modes not being as well confined (lower difference between refractive indices of the bulk and core). Generally, values below 0.5 dB/cm can still be expected.

These straight waveguides are the most basic building block for photonic circuits. They are commonly used to guide light without performing any particular transformation. However, through interaction with other waveguides, complex devices may be created.

Wave retarders

A wave retarder or waveplate is a fundamental component of optical systems. It changes the polarization of light while traveling through it. The relative phase change created is given by:

$$\Delta\phi = k_0 \Delta n d, \tag{2}$$

where $\Delta\phi$ is the phase change, Δn is the material birefringence and d is the thickness of the crystal.

To control how the waveguide affects the polarization, three parameters must be controlled. The birefringence, the optical axis and the length of the waveguide.

The birefringence value is the result of the fabrication process and material used. When using FLDW, typical values of $\Delta n \approx 10^{-5}$ [20] are expected when trying to minimize this effect. When trying to maximize it, values of the order of 10^{-4} [16] are usually obtained.

The optical axis is also a result of fabrication methods. Most waveguides are created with the fast axis along the vertical direction and the slow axis along the horizontal direction. Nevertheless, using techniques previously described, this can be changed and an almost arbitrary set of axis can be chosen.

The loss of this device can be modeled in the same way as a simple waveguide. In order to minimize the losses, the size must be minimized. However, in order to implement certain operations, a minimum length is required.

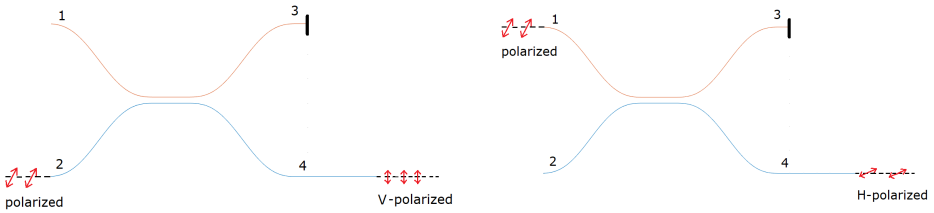

Figure 7: Example of how the polarizing beam coupler can be used to replace the polarizing beam splitter.

Curved waveguides

Bent waveguides are necessary in almost all photonic designs. They are important as input/output waveguides for different devices, for example, directional couplers. Because of distortions of the optical field that occur when guided waves travel through a bend in a channel waveguide, radiation loss can be greatly increased. In fact, the minimum allowable radius of curvature of a waveguide is generally limited by radiation losses rather than by fabrication tolerances.

The radiation loss in a curved waveguide decreases exponentially with the radius of the curve, equation 3. This means that there is a radius, R, for each waveguide for which the losses, α, due to bending can be made negligible.

$$\alpha = C_1 e^{(-C_2 R)}, \tag{3}$$

where C_1 and C_2 are constants that depend on the dimensions of the waveguide, and on the shape of the optical mode.

Directional coupler

Using curved waveguides, it becomes possible to develop new and more complex devices. For example, the directional coupler. In bulk optics, two beams can be overlapped into one spatial mode using a beamsplitter. In integrated optics, this task can be fulfilled by a directional coupler, which architecture is depicted in Fig 8.

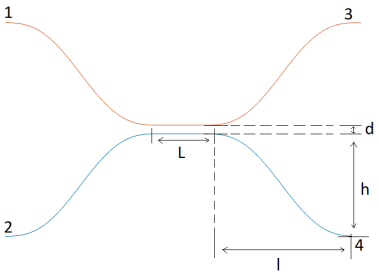

Figure 8: Design of a directional coupler with the control parameters represented.

Here, light coupled into port 1 will travel along the single mode waveguide and, as the waveguides get closer, light will be transferred to the other single mode waveguide by evanescent coupling.

If the waveguides are identical, coupling will continue until all power is in the opposite waveguide and past that distance, power will return to the original waveguide. This behavior is periodical and given by equations 4 and the interaction length defines the power splitting at the output ports 3 and 4.

$$\begin{aligned} A_1(z) &= \cos(Kz)e^{-i\beta z} \\ A_2(z) &= -i\sin(Kz)e^{-i\beta z} \end{aligned} \quad . \tag{4}$$

Polarizing Directional coupler

Previously, the analysis of a directional coupler device was done without considering birefringence. Nevertheless, the coupling strength, K, is dependent on the refractive index of the waveguide, which in turn is polarization dependent due to the intrinsic birefringence.

Considering K_V and K_H different due to this birefringence, the beat lengths of H and V modes differ, allowing to choose an optimal interaction length of the device corresponding to the distribution of orthogonally polarized states of light to distinct output modes of the coupler. This has been demonstrated by different teams, figure 9.

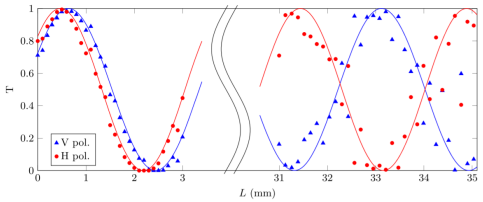

Figure 9: Experimental measurements of the transmission T of DCs with different interaction length L and waveguide separation d=12.5 μm, for H (red circles) and V (blue triangles) polarised input light. Solid lines are best-fitting theoretical curves.[16]

Then, the length can be chosen in order to act like a polarizing beamsplitter, figure 7.

5. Integrated photonic design for QKD

As explained before, using waveguides and the birefringent properties of materials, the polarization of light can be controlled while guiding it through waveguides. From figure 1, it can be seen that the essential optical elements needed to perform the BB84 protocol are mirrors, beam splitters, half-waveplates and polarizing beam splitters.

Equivalent elements in integrated optics have been design. Therefore, starting from the design using bulk optics, a similar design can be obtained with integrated optics.

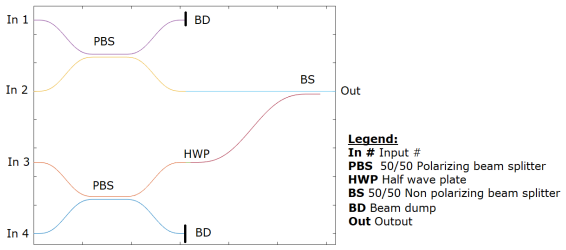

Figure 10: Schematic design of a possible integrated photonic circuit to reproduce the BB84 protocol.

The design in figure 10, illustrates how to reproduce figure 1 with the elements designed previously. There are still four inputs numbered from 1 to 4. The first input is followed by a polarizing directional coupler design with the intent of being a polarizing beam splitter. The light linearly polarized at this input will come out horizontally polarized at the output while from input 2, a vertically polarized state will come out. For this, the interaction length has to be carefully chosen as discussed before.

These two inputs are distanced from the other two in other not to interact. Input 3 and 4 go through an identical directional coupler and the same output follows. Nevertheless, on this side, a half-waveplate, created by a waveguide with a higher birefringence, rotates the polarization in order to create the diagonally and anti-diagonally polarized states.

Then, the two outputs are combined in the same output waveguide using a non-polarizing directional coupler. This way, each input corresponds to a different optical path and therefore, a different final state or polarization.

Figure 11 shows the integrated circuit in scale. On the y-axis, a distance of 125 μm was chosen because a VCSEL array with this distance between emitters was acquired as a potential replacement for the diode lasers.

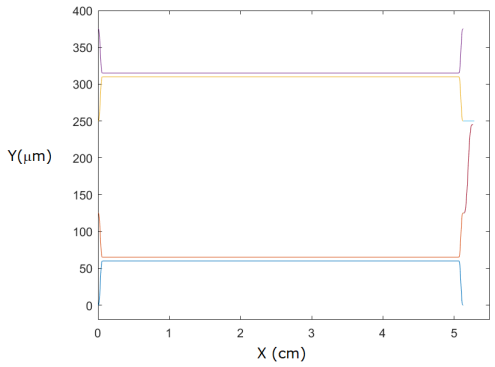

Figure 11: Same design as in figure 10 with the correct size and scale.

The size on the x-axis was determined by the length of the photonic elements. Most of the length of the device comes from the polarizing directional coupler. Due to the usual values of birefringence obtained, a significant size is required to reproduce the expected results.

With some assumptions made, a general estimate for the overall loss would be around 4.3 dB. In [15], the whole chip for tomography yields losses of 4.4 dB (including coupling losses, propagation and bending losses). The values are close to each other.

While this result is only a estimation taking into consideration different values in the literature, it allows to access the theoretical validity of the design. In this case, a total size of 52x0.5 mm^2 for the photonic circuit with a loss of 4.3 dB would result in a functional design and with a typical value for the overall loss. The size and weight (negligible) would allow for small scale applications like a nano-satellite.

6. Towards an efficient source of photon pairs

Until now, the source of single photons used was always based on weak coherent pulses. However, due to the acquisition of a PPKTP crystal, a new source can be made and different protocols explored. The reason for this is that PPKTP crystals can create spontaneous parametric down-conversion.

SPDC is a nonlinear optical process where a photon spontaneously splits into two other photons of lower energies. The most energetic photon is called the pump photon, while the resulting ones are called the signal and idler (for historical reasons).

Using Maxwell's equations for arbitrary dielectrics, the rate of change of the energy of the electromagnetic field U_{EM} can be expressed purely in terms of fields as:

$$\frac{dU_{EM}}{dt} = \int d^3r \left(\mathbf{H} \cdot \frac{d\mathbf{B}}{dt} + \mathbf{E} \cdot \frac{d\mathbf{D}}{dt} \right), \qquad (5)$$

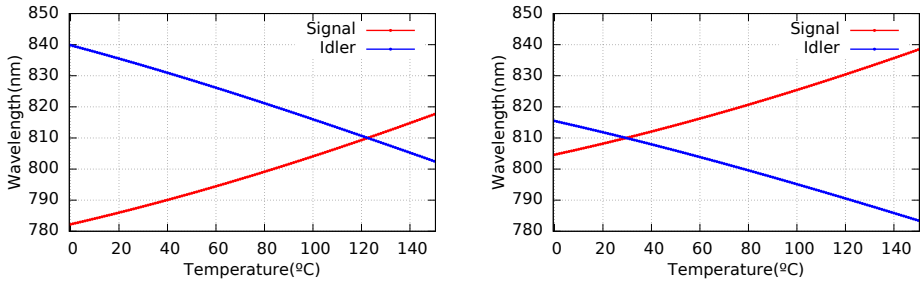

Figure 12: Theoretical phase matching curves for PPKTP samples. On the left, a period of $\Lambda = 10\,\mu m$. On the right $\Lambda = 10.35\,\mu m$.

where $\mathbf{D} = \epsilon_0\mathbf{E} + \mathbf{P}$, and $\mu_0\mathbf{H} = \mathbf{B} - \mu_0\mathbf{M}$. From this equation, the Hamiltonian of the SPDC process can be found. With the Hamiltonian defined, it is possible to find the state of the system. The amplitude of this state is:

$$\Pi(\lambda_s, \lambda_p - \lambda_s, \mathbf{q}_s, \mathbf{q}_i) = \sigma L_z \underbrace{\phi(\lambda_s, \lambda_p - \lambda_s)}_{\text{Spectral distribution}} \underbrace{\text{sinc}\left(\frac{\Delta k_z L_z}{2}\right)}_{\text{Phase matching}} \underbrace{G\Big(\mathbf{q}_s + \mathbf{q}_i\Big)}_{\text{Spatial distribution}}, \tag{6}$$

The probability of this state is only significant when there is energy and momentum conservation, the phase matching conditions. The energy conservation implies that $\lambda_i = \lambda_p - \lambda_s$. The momentum conservation comes from the sinc term, which is maximum when $\Delta k_z \approx 0$. $\Delta k_z = k_{pz} - k_{sz} - k_{iz}$

Quasi-phase matching

There are different ways to achieve the phase matching conditions. With a PPKTP crystal, instead of a homogeneous nonlinear crystal material, a material with spatially modulated nonlinear properties is used. With this propriety, the phase matching condition becomes:

$$\Delta k_z = k_{pz} - k_{sz} - k_{iz} - \frac{2\pi}{\Lambda} = 0. \tag{7}$$

With a new parameter, the poling period (Λ), the system can be tuned to maximize the state amplitude, its probability.

This leads to some clear advantages. First, the period Λ can be chosen such that collinear down-conversion is phase matched. This makes it much easier to collect the signal and idler photons produced.

Furthermore, the beams can be made to travel along one of the crystal's crystallographic axes. This then eliminates the problems caused by spatial walk-off, and therefore allows the use of much longer crystals, which again leads to an increased signal.

Temperature dependence

Using the Sellmeier equations to account for changes in the refractive index for different wavelengths and parabolic functions of temperature for the changes of the poling period and refractive index with temperature, simulations were used to calculate the wavelengths of SPDC emitted light as a function of temperature for slightly different poling periods, figure 12.

Typical PPKTP samples have a poling period of around $10\,\mu m$. As it can be seen in figure 12, the temperature for degenerate SPDC with an exact period of $10\,\mu m$ would be near 120ºC. In order to have a degenerate behaviour near room temperatures, the poling period has to be increased. When this value is $10.35\,\mu m$, the temperature is 29.58ºC.

From equation 6, the spectral density for a given value of $\mathbf{q}_s$ can be plotted as a function of wavelength. These numerically simulated tuning curves are done by integrating equation 6 in $\mathbf{q}_i$ for a given variable set $(\mathbf{q}_s, \lambda_s)$. The integration boundaries for $\mathbf{q_i}$ are limited to an empirically found range where the phase matching condition is fulfilled. The results showed here are for a Gaussian beam assumption.

From figure 13, it can be seen that while the behaviour for different values of $|\mathbf{q_s}|$ is the same, as it increases, the maximum value of the spectral emission moves away from the degenerate wavelength. The emission signal is almost symmetric around a central wavelength with slight differences in the oscillations, most likely due to the difference in refractive index as a function of wavelength. Nevertheless, the typical behaviour of the sinc function is clearly seen in these small oscillations after the decay.

From the result for distinct values of $|\mathbf{q_s}|$, it follows that in different directions, the most commonly emitted frequency is different. This gives rise to colored emission rings.

Currently, the PPKTP crystal is being characterized in order to create a reliable and efficient source of photon pairs. These photon pairs can then be used as a heralded single photon source or for en-

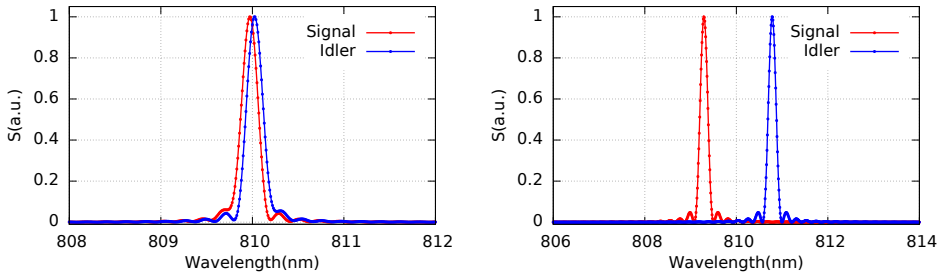

Figure 13: Normalized simulated spectral densities for two different values of $|\mathbf{q_s}|$ and a fixed value of temperature. On the left $|\mathbf{q_s}| = 0\,\mu m^{-1}$, on the right $|\mathbf{q_s}| = 0.2\,\mu m^{-1}$

tanglement generation. Both application will be explored in future work for a variety of projects.

7. Conclusions

This work proposes an integrated photonic design for quantum key distribution. The design is small enough for the applications in mind (52×0.5 mm^2). Furthermore, the estimations of the device's losses (4.3 dB) are not prohibitive of its use. However, no prototype was created and characterized. Although similar projects exist in the literature and work, it can not be concluded that this design will perform as expected.

In this project, a different fabrication method was also pursued. By studying and discussion its advantages and disadvantages, it was established as a reliable method with much potential. Nevertheless, its initial cost is high and alternatives to buying a femtosecond laser are being explored.

Moreover, the characterization process of a PPKTP is underway. As the initial tests were inconclusive, a more in depth analysis was necessary. Therefore, a systematic characterization of the elements and a complete theoretical study of the crystal was done. This has pointed to new ideas that will be explored in the future.

All in all, the work developed here was a necessary step forward in bigger projects for the Quantum Technologies group.

References

[1] C. H. Bennett, G. Brassard, *Theoretical Computer Science* **560**, 7–11 (2014).

[2] Quantum technologies flagship, `https://ec.europa.eu/digital-single-market/en/quantum-technologies-flagship` (2020).

[3] E. Diamanti, H.-K. Lo, B. Qi, Z. Yuan, *npj Quantum Information* **2**, 1 (2016).

[4] E. Gibney, *Nature* **535**, 478—479 (2016).

[5] J. Yin, *et al.*, *Science* **356**, 1140 (2017).

[6] S. P. Neumann, *et al.*, *EPJ Quantum Technology* **5**, 4 (2018).

[7] D. K. L. Oi, *et al.*, *Contemporary Physics* **58**, 25 (2017).

[8] J. Matthews, A. Politi, A. Stefanov, J. O'Brien, *Nature Photonics* **3**, 346 (2009).

[9] T. K. Paraïso, *et al.*, *NPJ Quantum Information* **5**, 42 (2019).

[10] G. D. Marshall, *et al.*, *Optics express* **17**, 12546 (2009).

[11] G. Mélen, Integrated quantum key distribution sender unit for hand-held platforms, Ph.D. thesis, lmu ((2016)).

[12] P. W. Shor, J. Preskill, *Physical review letters* **85**, 441 (2000).

[13] K. Itoh, W. Watanabe, S. Nolte, C. Schaffer, *MRS Bulletin* **31** (2006).

[14] U. Haken, O. Humbach, S. Ortner, H. Fabian, *Journal of Non-Crystalline Solids* **265**, 9 (2000).

[15] G. Corrielli, *et al.*, *Nature communications* (2014).

[16] I. Pitsios, F. Samara, G. Corrielli, A. Crespi, R. Osellame, *Scientific Reports* (2017).

[17] E. N. Glezer, E. Mazur, *Applied Physics Letters* **71**, 882 (1997).

[18] S. Gross, M. J. Withford, *Nanophotonics* **4**, 332 (2015).

[19] C. B. Schaffer, J. F. García, E. Mazur, *Applied Physics A* **76**, 351 (2003).

[20] L. A. Fernandes, J. R. Grenier, P. R. Herman, J. S. Aitchison, P. V. S. Marques, *Opt. Express* **19**, 11992 (2011).